

# Silicon carbide fibre reinforced glass-ceramic matrix composites exhibiting high strength and toughness

JOHN J. BRENNAN, KARL M. PREWO

*United Technologies Research Center, East Hartford, CT 06109, USA*

Silicon carbide fibre reinforced glass-ceramic matrix composites have been investigated as a structural material for use in oxidizing environments to temperatures of 1000° C or greater. In particular, the composite system consisting of SiC yarn reinforced lithium aluminosilicate (LAS) glass-ceramic, containing ZrO<sub>2</sub> as the nucleation catalyst, has been found to be reproducibly fabricated into composites that exhibit exceptional mechanical and thermal properties to temperatures of approximately 1000° C. Bend strengths of over 700 MPa and fracture toughness values of greater than 17 MN m<sup>-3/2</sup> from room temperature to 1000° C have been achieved for unidirectionally reinforced composites of ~ 50 vol% SiC fibre loading. High temperature creep rates of 10<sup>-5</sup> h<sup>-1</sup> at a temperature of 1000° C and stress of 350 MPa have been measured. The exceptional toughness of this ceramic composite material is evident in its impact strength, which, as measured by the notched Charpy method, has been found to be over 50 times greater than hot-pressed Si<sub>3</sub>N<sub>4</sub>.

## 1. Introduction

During the past few years, United Technologies Research Center (UTRC) has been conducting several research programmes in the area of glass matrix composites reinforced with graphite [1-3], alumina [4], and SiC fibres [5, 6]. In all of these programmes it was found that the use of fibres exhibiting high strength and stiffness was successful in reinforcing low modulus glass matrices. In particular, for high temperature use in an oxidizing atmosphere, it was demonstrated that the SiC fibre reinforced glass matrix composite system was capable of achieving excellent mechanical properties up to 600° C [5]. Both SiC monofilament (supplied by AVCO Corp.) and SiC yarn (supplied by Nippon Carbon Co.) were evaluated in a borosilicate glass (Corning 7740) matrix. While this system resulted in exceptionally high fracture toughness and flexure strength to 600° C, to fully utilize the high temperature potential of the SiC fibre reinforcement, a higher temperature matrix than 7740 glass must be utilized.

The more recent development of high silica

glass matrix composites [6] was in response to this need for higher thermal stability. Although achieving higher use temperatures this approach also resulted in significantly greater fabrication difficulties due to the much higher viscosity of the higher temperature glass during composite consolidation. The use of a glass-ceramic as composite matrix, however, can result in a combination of high composite use temperature and also fabrication ease. Composite densification can occur while the matrix is maintained in a low viscosity glass state while composite structural use can take place after the matrix has been crystallized for thermal stability.

The main objective of the present study was the development of a high strength, high toughness, low density SiC fibre reinforced glass or glass-ceramic matrix composite that has a use temperature of at least 1000° C. The achievement of this objective has been explored through the unique approach of using oxide glass-ceramics as the matrices for reinforcement. The use of a matrix in the glassy state was essential to the success of

this effort in that glasses provide the following advantages.

(a) A glass matrix, because of its viscous flow characteristics, can be densified at elevated temperatures without damage to any reinforcing fibres. This is in contrast to crystalline ceramics where densification under pressure can lead to fibre damage.

(b) Most glasses and glass-ceramics have elastic moduli in the range of 60 to 100 GPa (10 to  $15 \times 10^6$  psi). These values are significantly lower than those of many reinforcing fibres. Hence, these matrices can be structurally reinforced by transfer of load from the matrix to the fibres.

(c) The densities of many glasses and glass-ceramics are low, 2.2 to  $2.7 \text{ g cm}^{-3}$ , so that resultant composite densities are low.

(d) Glasses and glass-ceramics can exhibit physical/chemical stability well above  $1000^\circ \text{C}$ .

(e) Glass-ceramics provide the unique capability to densify a composite in the glassy stage and then subsequently crystallize the matrix to achieve high temperature stability.

## 2. Materials

The SiC fibre used throughout this study is that produced by Nippon Carbon Co. in Japan and sold in the USA by Sumitomo Shoji, Inc., New York, NY. These fibres are available in continuous length (about 500 m) tows of 500 fibres per tow with an average diameter of  $12 \mu\text{m}$ . The average tensile strength and elastic modulus of this fibre, as measured at UTRC, is 2060 MPa and 206 GPa, respectively.

The matrix material used in this study is essentially identical to Corning Glass Works' commercial 9608 lithium aluminosilicate (LAS), except that the  $\text{TiO}_2$  nucleating agent was replaced by a  $\text{ZrO}_2$  nucleating agent. The LAS glass-ceramic matrix was chosen as the only viable glass candidate that could be densified at a reasonable temperature ( $< 1600^\circ \text{C}$ ) and still allow a use temperature of at least  $1000^\circ \text{C}$ , due to its ability to be fabricated in a low viscosity glassy state with subsequent transformation into a more refractory crystalline state. The LAS matrix material was received from Corning Glass Works in a glassy powder of approximately  $12 \mu\text{m}$  average particle size.

## 3. Composite fabrication

The SiC yarn-LAS glass-ceramic composites were fabricated by passing the SiC yarn through an

agitated slurry of the glass powder and isopropyl alcohol onto a rotating drum, drying the resultant tape and then cutting the tapes into the appropriate length to fit the hot-pressing die. After the tapes were cut to length, sufficient tape was stacked in the die to obtain the desired thickness composite and then the assembly was hot-pressed in vacuum at temperatures greater than  $1300^\circ \text{C}$  under applied pressures greater than 6.9 MPa. The resulting composite plates were  $7.6 \text{ cm} \times 7.6 \text{ cm}$  square with thicknesses ranging from 1.9 mm to 6.3 mm. The pressed composites were then weighed and measured for density determinations and then cut into the appropriate test configuration. Those samples to be tested in the crystalline state were then "ceramed" or heat-treated for 1 to 2 h at maximum temperatures of  $880^\circ \text{C}$  to  $1100^\circ \text{C}$ . Pieces of each composite were also examined metallographically and by X-ray diffraction in order to determine the amounts of glassy and crystalline phases present after the hot-pressing and "ceraming" steps.

Fig. 1 shows the cross-sections of a unidirectionally reinforced and a  $0^\circ/90^\circ$  cross-plyed LAS-SiC composite. The volume fraction of SiC fibres is approximately 50% in both samples. In the cross-plyed sample, the per-ply thickness averages  $220 \mu\text{m}$  so that a normal 13 ply composite plate is  $\sim 3 \text{ mm}$  thick. The samples exhibit essentially zero porosity with bulk density of  $\sim 2.5 \text{ g cm}^{-3}$ . Note that the Nippon Carbon SiC fibres vary considerably in diameter, as shown in Fig. 1, with some being as small as  $5 \mu\text{m}$  and a few as large as  $60 \mu\text{m}$ .

## 4. Composite mechanical properties

### 4.1. Flexural strength

The flexural strength of both  $0^\circ$  and  $0^\circ/90^\circ$  SiC-LAS composites was measured in three-point bending as a function of temperature from room temperature (r.t.) to  $1200^\circ \text{C}$ . Sample dimensions were approximately 2.5 mm thick by 5 mm wide with a 63 mm span. All samples were tested in the "ceramed" condition since after hot-pressing the matrix was in the glassy state. Ceraming was accomplished by heating the composite samples in air to  $780^\circ \text{C}$  for 2 h, raising the temperature at  $250^\circ \text{C h}^{-1}$  to 880 to  $1100^\circ \text{C}$  and holding for 1 to 2 h. From X-ray diffraction analysis of crushed samples after ceraming, the matrix contained substantial amounts of crystalline lithium aluminosilicate usually in the  $\beta$ -quartz solid solution phase  $[(\text{Li}_2\text{O}, \text{MgO}) \cdot \text{Al}_2\text{O}_3 \cdot n\text{SiO}_2 (n \geq 2)]$ .

*Figure 1* Cross-section of LAS–SiC (a) unidirectional and (b)  $0^\circ/90^\circ$  cross-plyed yarn composites.

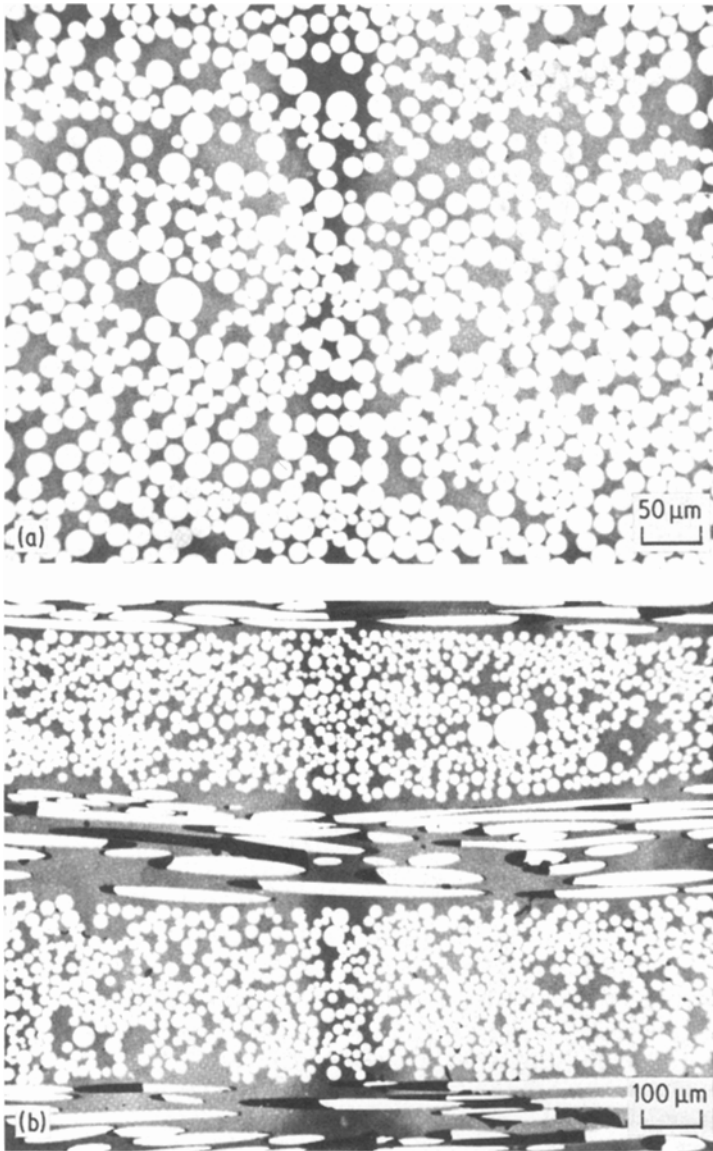


Fig. 2 shows the flexural strength for LAS–SiC composites as a function of temperature for both the unidirectional ( $0^\circ$ ) and cross-plyed ( $0^\circ/90^\circ$ ) fibre alignment. Also shown is the strength of monolithic LAS (Corning 9608). Each point on the curves represents the average of at least five tests, with the r.t. tests representing over 15 samples. At elevated temperatures the spread in flexural strength values from sample to sample was very low while at r.t. it was considerably greater, especially for the  $0^\circ$  orientation composites, as shown in Fig. 2. The unidirectionally reinforced composite samples exhibit bend strengths of over 620 MPa at r.t., increasing to over 830 MPa at

$900\text{--}1000^\circ\text{C}$ . Cross-plyed samples ( $0^\circ/90^\circ$ ) exhibit strengths of over 350 MPa at r.t. and 480 MPa at  $1000^\circ\text{C}$ . The reason for the increase in strength with increasing temperature is that the viscosity of the glass is decreasing, thus increasing its strain capacity. Above about  $1050^\circ\text{C}$  the effective flexural strength of the composite drops off due to the residual glassy phase within the matrix becoming too low in viscosity to effectively transfer load to the fibres. At  $1200^\circ\text{C}$  the matrix deforms completely plastically with the result that the composite does not fracture, but simply bends into a “V” shape. Because of this large deformation the value of strength calculated is

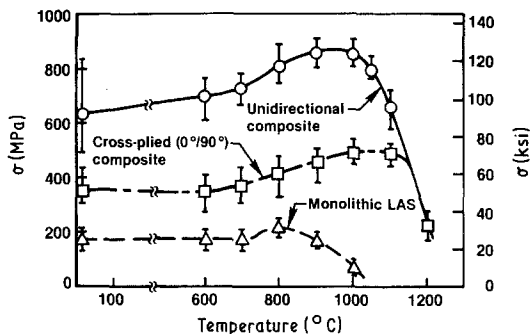


Figure 2 Flexural strength (three-point) for LAS-SiC yarn composites.

inaccurate; however, it does express the change in load bearing capacity of the composite. In contrast to the LAS-SiC composites, monolithic 9608 LAS exhibits a bend strength of less than 200 MPa ( $30 \times 10^3$  psi) from r.t. to 900°C with very little useful strength at 1000°C.

The stress-strain curve for the LAS-SiC composite material in the ceramed condition is essentially linear up to  $\sim 1050^\circ\text{C}$ , indicative of the refractory nature of the glass-ceramic matrix in the crystalline condition. In addition, when the composite material fractures, it does not fail completely but remains in one piece that is still capable of carrying substantial load. The monolithic LAS material, in contrast, breaks into two pieces upon fracture. If the composite material is stressed sufficiently to finally fracture it, the fracture surface is very brushy in appearance, with a large amount of fibre pullout as shown in Fig. 3. The fibre pullout is indicative of fairly weak fibre to matrix bonding, which is very important for high fracture toughness, as will be discussed later in this article.

#### 4.2. Elastic modulus

The elastic or Young's modulus of both the  $0^\circ$  and  $0^\circ/90^\circ$  composite material and monolithic LAS were measured from r.t. to 1200°C. The composite values at r.t. were measured both in tension, utilizing strain gauges, and in bending from the load-deflection curves. The agreement between the two methods was quite good. Elevated temperature values were measured in bending from the load-deflection traces.

Fig. 4 shows the elastic modulus against temperature curves for the composite material and monolithic LAS. With a measured SiC fibre modulus of 210 GPa ( $30 \times 10^6$  psi), the composite

values are very close to that predicted from the rule of mixtures.

#### 4.3. Fracture toughness

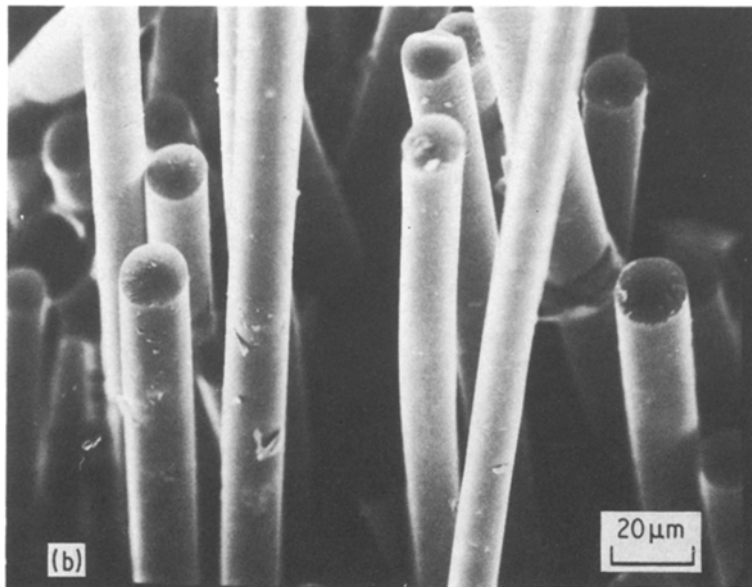
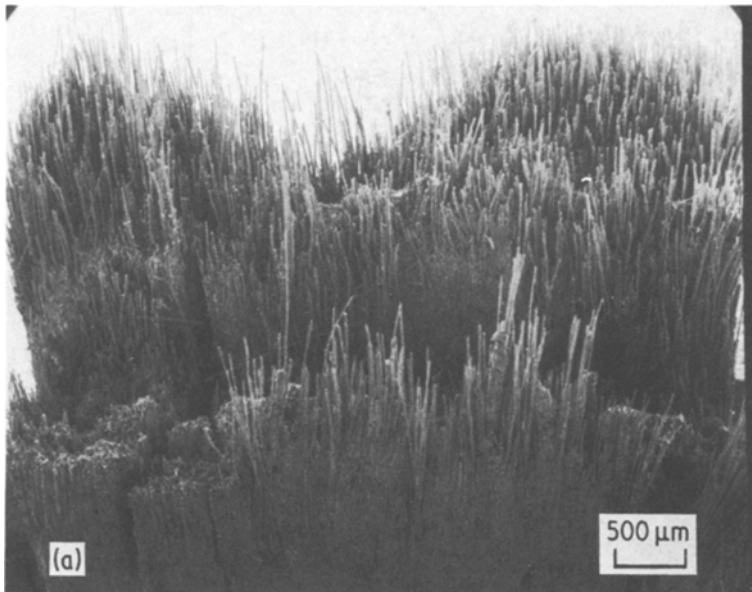
The fracture toughness, as expressed by the critical stress intensity factor ( $K_{IC}$ ), of the SiC-LAS composite system and monolithic LAS was measured from r.t. to 1100°C using the notched beam method. This test was selected to provide a measurement of  $K_{IC}$  values due to the much greater ease of sample preparation over that necessary for such methods as the double torsion or cantilever beam. Sample dimensions were 0.635 cm square by 7.5 cm long with a span of 6.35 cm. A 150  $\mu\text{m}$  thick diamond saw blade was used to form the tip of the notch in the specimens. The notch depth to sample thickness ratio was 0.5 in all cases. The value of  $K_{IC}$  was calculated from the equation formulated by Brown and Srawley [7].

Fig. 5 shows the  $K_{IC}$  values against temperature for  $0^\circ$  and  $0^\circ/90^\circ$  SiC-LAS composites in the ceramed condition and for monolithic Corning 9608 LAS. The unidirectionally reinforced composite samples exhibit  $K_{IC}$  values of  $17 \text{ MN m}^{-3/2}$  at r.t., increasing to  $25 \text{ MN m}^{-3/2}$  at 1000°C, while the  $0^\circ/90^\circ$  cross-plyed samples exhibit  $K_{IC}$  values of over  $10 \text{ MN m}^{-3/2}$  from r.t. to 1000°C. Even hot-pressed Norton Co. NC-132  $\text{Si}_3\text{N}_4$ , one of the toughest monolithic ceramics, possesses a  $K_{IC}$  of only  $4.5 \text{ MN m}^{-3/2}$  at r.t., as measured at UTRC. The r.t.  $K_{IC}$  value of  $17 \text{ MN m}^{-3/2}$  for the  $0^\circ$  SiC-LAS composite system is not significantly different from the r.t.  $K_{IC}$  of 2024-T6 aluminium alloy of  $22 \text{ MN m}^{-3/2}$  and about half that of  $0^\circ$  graphite-epoxy composite material ( $34 \text{ MN m}^{-3/2}$ ) which is used extensively in many commercial and military structural applications [8].

Fig. 6 shows the load-deflection curves for the  $0^\circ$  and  $0^\circ/90^\circ$  LAS-SiC composites and monolithic 9608 LAS, for the r.t. notched beam  $K_{IC}$  tests. The very large deflection before load drop-off for the composite materials is indicative of their excellent strain capability, compared to monolithic ceramics. The change in slope of the composite load-deflection curves at approximately one-half of the maximum load represents the onset of matrix microcracking. Many graphite-epoxy composites also exhibit this type of behaviour.

Fig. 7 shows a  $0^\circ$  and a  $0^\circ/90^\circ$  SiC-LAS notched beam sample after  $K_{IC}$  testing. The propagation of

Figure 3 Room temperature fracture surfaces of LAS–SiC yarn composite.



cracks along the fibre–matrix interfaces can be seen with the help of Zyglodye penetrant. These samples have been deflected well beyond the point of maximum load and yet are still in one piece. The cracks propagating from the notch tip have yet to reach the compression side of the sample. In contrast, the monolithic LAS  $K_{IC}$  specimens broke in half immediately after maximum load was attained. The practical significance of this can be demonstrated by dropping a plate of monolithic LAS and a plate of  $0^\circ/90^\circ$  cross-plyed LAS–SiC composite on a hard surface. The monolithic LAS

will shatter into many pieces whereas the LAS–SiC composite will simply bounce.

#### 4.4. Charpy impact

In order to assess the effect of a much faster loading rate ( $\sim 10^5$  times that for a  $K_{IC}$  test) on the toughness of LAS–SiC composites, Charpy impact tests were run at r.t. and  $800^\circ\text{C}$  on notched and unnotched  $0^\circ$  and  $0^\circ/90^\circ$  cross-plyed composites. The notched samples had exactly the same configuration as those used for  $K_{IC}$  tests, i.e. the notch depth–sample thickness was  $\sim 0.5$ . For

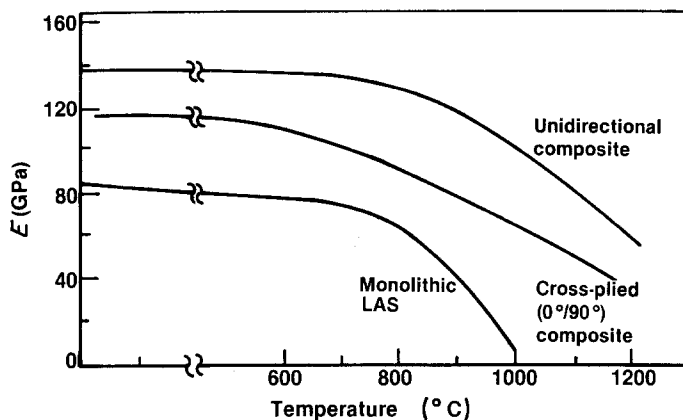


Figure 4 Elastic modulus of LAS-SiC yarn composites.

comparison, samples of NC-132  $\text{Si}_3\text{N}_4$ , notched and unnotched of identical size,  $6.4 \times 6.4 \times 45$  mm were also impacted.

The results of these tests are presented in Table I. It can be seen that a  $0^\circ$  composite exhibits approximately three times the impact energy of a  $0^\circ/90^\circ$  cross-plyed composite in the unnotched condition, and twice the energy in the notched condition. There does not appear to be any significant difference between the samples tested at r.t. and  $800^\circ\text{C}$ . On an impact energy per cross-sectional area basis, the  $0^\circ/90^\circ$  cross-plyed samples are quite similar whether notched or unnotched, indicating that this material is very notch insensitive. The  $0^\circ$  composite appears to be slightly notch sensitive. Neither the  $0^\circ$  or  $0^\circ/90^\circ$  LAS-SiC composite is sensitive to loading rate, since the maximum load to failure for the material in the notched configuration is approximately the same whether loaded at  $0.025 \text{ cm min}^{-1}$  for  $K_{\text{IC}}$  testing or at  $5.5 \times 10^3 \text{ cm min}^{-1}$  for Charpy impact testing.

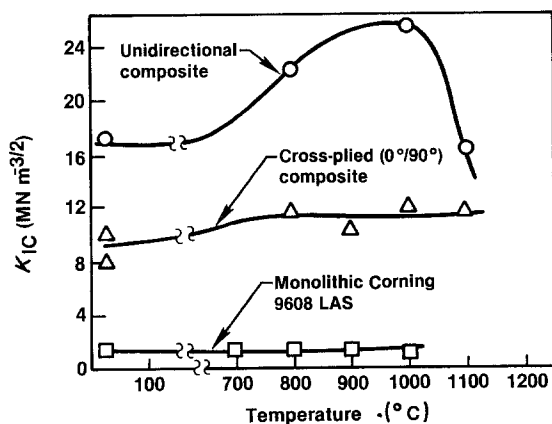


Figure 5 Fracture toughness,  $K_{\text{IC}}$ , of LAS-SiC yarn composites.

In comparison to NC-132  $\text{Si}_3\text{N}_4$ , in the unnotched condition the LAS-SiC composite material is almost five times as impact resistant in the  $0^\circ$  configuration and slightly more impact resistant in the  $0^\circ/90^\circ$  configuration. However, in the notched condition, the  $0^\circ$  composite material is over 50 times as impact resistant as  $\text{Si}_3\text{N}_4$  while the  $0^\circ/90^\circ$  composite is almost 30 times as impact resistant. This is a good illustration of the advantages of this type of ceramic composite material over an extremely notch sensitive monolithic ceramic such as hot-pressed  $\text{Si}_3\text{N}_4$ . The difference in fracture surfaces of these two materials tested in Charpy impact in the notched condition is shown in Fig. 8. While the NC-132  $\text{Si}_3\text{N}_4$  fracture surface is extremely flat and featureless, the LAS-SiC composite fracture surface is very jagged and rough with a large amount of fibre pullout occurring.

The fracture path in the LAS-SiC composite sample was obviously very tortuous, necessitating a large amount of energy to be expended during the impact event. In comparison, very little energy was necessary to propagate the crack front through the prenotched hot-pressed  $\text{Si}_3\text{N}_4$  sample.

#### 4.5. Elevated temperature creep

Creep tests in bending (three-point) at temperatures of  $700^\circ\text{C}$  to  $1100^\circ\text{C}$  and applied stresses of 140, 240 and 345 MPa have been performed on unidirectionally reinforced LAS-SiC composite samples in the ceramed condition. Sample dimensions were  $2.54 \times 5.08 \times 63.5$  mm span. From the results of these tests, it was found that no measurable creep occurred at either  $700^\circ\text{C}$  or  $800^\circ\text{C}$ . At  $900^\circ\text{C}$ , a very low steady state creep rate was observed, as shown in Fig. 9. Not until the temperature reached  $1100^\circ\text{C}$  did the observed rate of creep become

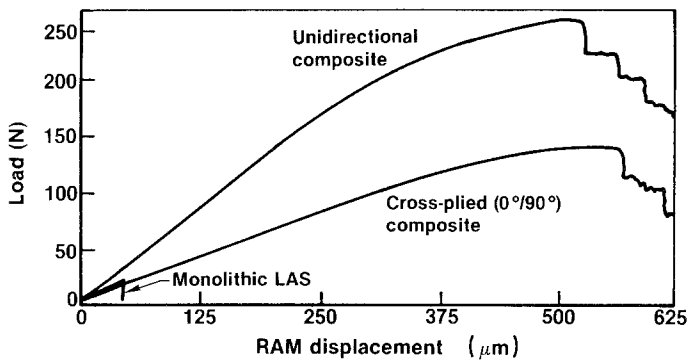


Figure 6 Room temperature notched beam load against deflection curves for LAS-SiC yarn composites.

significant. In all cases, tests were normally run for 24 h with steady state creep being attained in  $\sim 10$  h.

The stress exponent,  $n$ , from the creep equation

$$\dot{\epsilon} = A\sigma^n \exp(-E/kT) \quad (1)$$

where  $\dot{\epsilon}$  is the steady state creep rate,  $\sigma$  is the applied stress,  $E$  is the activation energy for creep,  $k$  is Boltzmann's constant,  $T$  is the temperature, and  $A$  is a constant, is very low ( $\sim 0.4$ ) for the tests conducted at  $900^\circ\text{C}$  and  $1000^\circ\text{C}$  and rather high (1.7) for the tests conducted at  $1100^\circ\text{C}$ , indicative of different creep mechanisms operable at these temperatures. Stress exponents of about 1 or less are generally associated with a diffusional creep mechanism while exponents of about 2 are associated with deformation being controlled by the viscoelastic behaviour of glassy grain boundary phases. A stress exponent of 0.3 has previously been found for hot-pressed SiC

[9]. It would appear then, that for the current LAS-SiC composites under investigation, creep at temperatures of approximately  $1000^\circ\text{C}$  or less may be controlled by diffusional creep of the SiC fibres or the LAS matrix while at  $1100^\circ\text{C}$  the residual glassy phase present in the matrix may control the creep deformation.

## 5. Composite thermal properties

### 5.1. Thermal expansion

The thermal expansion of LAS-SiC composites was measured in the axial ( $0^\circ$ ) and transverse ( $90^\circ$ ) directions over the temperature range of  $20^\circ\text{C}$  to  $1000^\circ\text{C}$ . Composite thermally induced strain was measured as a function of temperature with the average values of coefficient of thermal expansion calculated at  $2.2 \times 10^{-6} \text{C}^{-1}$  for the axial direction and  $1.6 \times 10^{-6} \text{C}^{-1}$  for the transverse direction.

Using Equations 53 and 62 from [10] for  $\alpha_{11}$

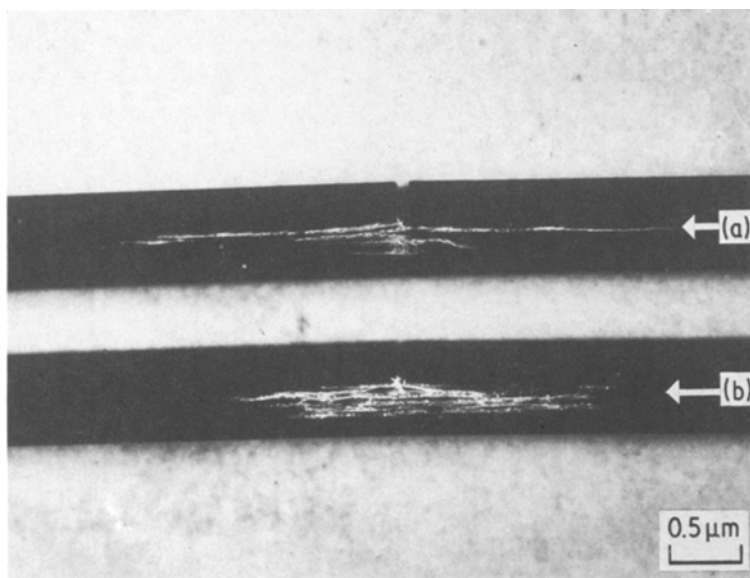


Figure 7 Room temperature LAS-SiC yarn notched beam samples (Zygo penetrant enhanced) for (a) unidirectional and (b)  $0^\circ/90^\circ$  cross-plyed composites.

TABLE I Charpy impact properties of LAS-SiC composites (6.4 mm × 6.4 mm × 45 mm span)

Sample	Fibre orientation	Temperature (°C)	Notch depth (mm)	Impact energy	
				(J)	(J cm <sup>-2</sup> )
LAS-SiC	0°	r.t.	no notch	1.84	4.57
		800		1.41	3.50
		r.t.	3.2	0.55	2.75
		800		0.72	3.60
	0°/90°	r.t.	no notch	0.61	1.50
		800		0.41	1.02
		r.t.	3.2	0.27	1.35
		800		0.26	1.30
NC-132	—	r.t.	no notch	0.40	0.98
Si <sub>3</sub> N <sub>4</sub>	—	r.t.	2.8	0.01	0.05

and  $\alpha_{22}$  for composites reinforced with isotropic fibres and using values of  $\alpha_f = 3 \times 10^{-6} \text{ C}^{-1}$ ,  $\alpha_m = 1 \times 10^{-6} \text{ C}^{-1}$ ,  $E_f = 30 \times 10^6 \text{ psi}$  (210 GPa), and  $E_m = 12.5 \times 10^6 \text{ psi}$  (85 GPa), and the predicted values of axial and transverse thermal expansion are  $2.4 \times 10^{-6} \text{ C}^{-1}$  and  $1.9 \times 10^{-6} \text{ C}^{-1}$ , respectively. Thus the agreement between predicted and measured values of  $\alpha$  for the LAS-SiC composite material is quite good.

The value of the matrix thermal expansion coefficient used in the above prediction is that given [11] for a fully crystallized LAS matrix of  $\beta$ -spodumene ( $\text{Li}_2\text{O} \cdot \text{Al}_2\text{O}_3 \cdot 4\text{SiO}_2$ ). This value can be even lower for  $\beta$ -spodumene-silica solid solutions, i.e.  $5 \times 10^{-7} \text{ C}^{-1}$  for  $\text{Li}_2\text{O} \cdot \text{Al}_2\text{O}_3 \cdot 6\text{SiO}_2$ , or somewhat higher if the matrix retains a substantial amount of glassy phase. Thus, the composite thermal expansion, especially in the transverse

direction, will be very sensitive to matrix chemical composition and crystallization behaviour.

## 5.2. Thermal conductivity

The thermal conductivity, or more specifically the thermal diffusivity, of the LAS-SiC fibre composite material was measured at r.t. through the use of the laser flash technique. These tests were performed by Professor D. P. H. Hasselman of the Dept. of Materials Engineering at Virginia Polytechnic Institute, Blacksburg, VA. The samples supplied to Professor Hasselman were in the form of 1.27 cm squares of  $\sim 1.25 \text{ mm}$  thickness. Fibre orientations were either 0° or 0°/90° with fibre volume fractions varying from 30% to 50%. Measurements were made both parallel and perpendicular to the fibre direction.

The results of these tests are given in Table II.

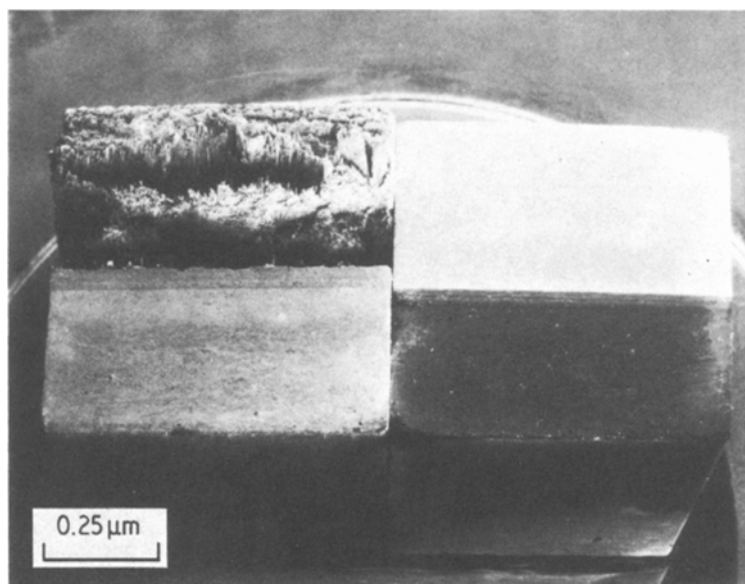


Figure 8 RT notched Charpy impact fracture surfaces of LAS-SiC 0° composite (left) and NC-132 Si<sub>3</sub>N<sub>4</sub> (right).



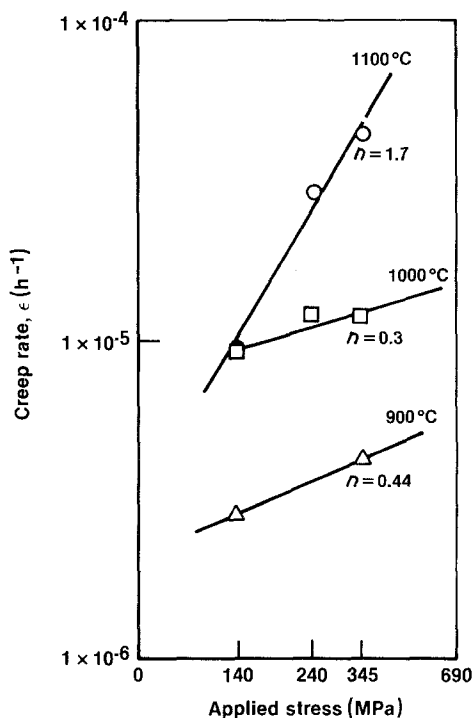


Figure 9 Steady-state creep rate in bending for LAS-SiC composites.

It appears from these results that, within experimental accuracy, the thermal diffusivity of r.t. of LAS-SiC composites, regardless of fibre volume fraction or orientation, is approximately the same as monolithic Corning 9608 LAS. Thus, the thermal diffusivity of the Nippon Carbon SiC fibres is very close to that of the LAS matrix. The value measured for the monolithic Corning 9608 LAS ( $0.0075 \text{ cm}^2 \text{ sec}^{-1}$ ) is somewhat lower than that given in the literature [11] of  $\sim 0.0100 \text{ cm}^2 \text{ sec}^{-1}$ .

Thermal diffusivity is related to thermal conductivity by the relationship:

$$K = \frac{k}{\rho C_p} \quad (2)$$

where  $K$  = thermal diffusivity,  $k$  = thermal conductivity,  $\rho$  = density and  $C_p$  = true specific heat. Thus, the thermal conductivity is given by the product of thermal diffusivity, density, and specific heat. The density of the 9608 type LAS matrix material is  $2.42 \text{ g cm}^{-3}$  while that of the SiC yarn is  $2.6 \text{ g cm}^{-3}$ . The specific heat of 9608 LAS at r.t. is  $\sim 0.19 \text{ cal g}^{-1} \text{ }^\circ \text{C}^{-1}$  ( $0.80 \text{ J g}^{-1} \text{ }^\circ \text{C}^{-1}$ ) [11] while that of the SiC yarn was measured by Professor Hasselman by differential scanning calorimetry to be  $\sim 0.67 \text{ J g}^{-1} \text{ }^\circ \text{C}^{-1}$ . Thus, the value of  $\rho C_p$  for the matrix is approximately the same as that for the fibre.

If the above assumptions are valid, then the r.t. thermal conductivity of the present LAS-SiC composite material, regardless of fibre volume fraction or orientation, can be approximated rather closely by that determined for the 9608 LAS matrix alone. This value at r.t. is  $\approx 0.0035 \text{ cal sec}^{-1} \text{ cm}^{-1} \text{ }^\circ \text{C}^{-1}$  ( $1.465 \text{ W m}^{-1} \text{ K}^{-1}$ ). Again, this value is somewhat less than that given in the literature [11] for 9608 LAS of  $0.0047 \text{ cal sec}^{-1} \text{ cm}^{-1} \text{ }^\circ \text{C}^{-1}$  ( $1.97 \text{ W m}^{-1} \text{ K}^{-1}$ ). Thus, the LAS-SiC composite system is a relatively good insulator, being lower in thermal conductivity than hot-pressed  $\text{Si}_3\text{N}_4$  and pure  $\text{Al}_2\text{O}_3$  by a factor of about 15, and lower than most nickel based super-alloys by a factor of about 7. It is, however, somewhat higher than good thermal insulators such as zirconia and fused silica by a factor of 1.5 to 2.

### 5.3. Thermal ageing

During studies dealing with the crystallization or "ceraming" behaviour of LAS-SiC composites, it was noted that samples heat-treated at maximum temperatures in air of over approximately  $950^\circ \text{C}$  for times of a few hours or more developed a rather thick glaze-like layer on the exposed surfaces. While it was found that a  $900^\circ \text{C}$  heat-

TABLE II Thermal diffusivity ( $K$ ) measurements for LAS-SiC composites

Sample	Fibre content (vol %)	Fibre orientation	$K$ measurement direction	$K$ ( $\text{cm}^2 \text{ sec}^{-1}$ )*
Corning 9608 LAS	—	—	—	0.0075
LAS-SiC	50	$0^\circ$	$\perp$ to fibres	0.0075
	30	$0^\circ$	$\perp$ to fibres	0.0073
	50	$0^\circ/90^\circ$	$\perp$ to fibres	0.0073
	35	$0^\circ/90^\circ$	$\perp$ to fibres	0.0073
	50	$0^\circ$	$\parallel$ to fibres	0.0080
	45	$0^\circ/90^\circ$	$\parallel$ to $0^\circ$ fibres	0.0075
			$\perp$ to $90^\circ$ fibres	

\*All values are averages of at least three tests.

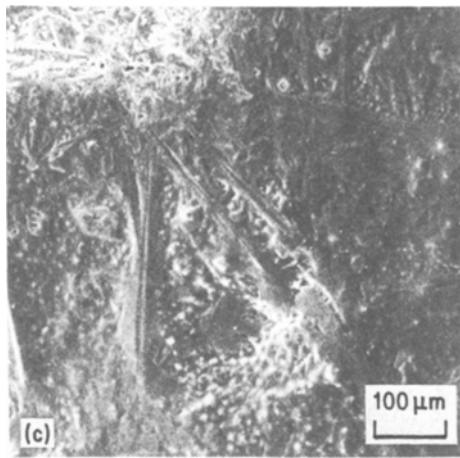
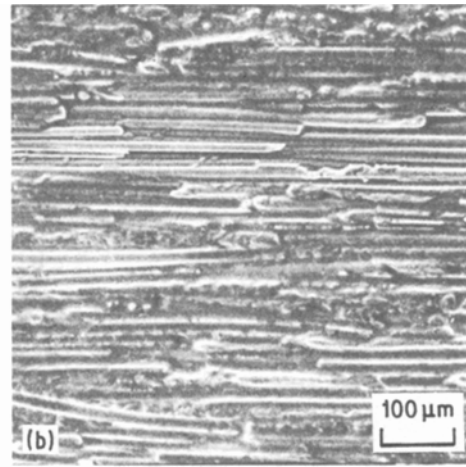
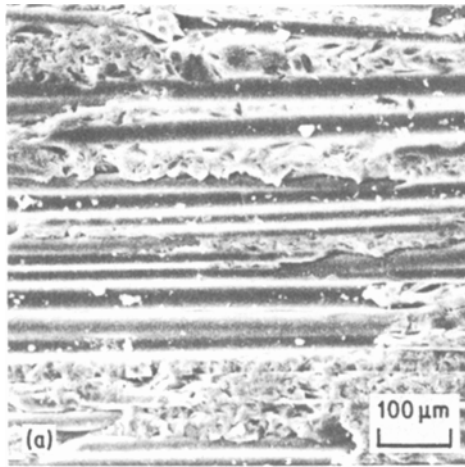


Figure 10 Surfaces of LAS-SiC composites (a) as-ground, (b) aged at 900° C for 2 h and (c) aged at 1050° C for 2 h.

treatment was sufficient for matrix crystallization, the appearance of this surface glaze at temperatures below the potential composite use temperature was somewhat disturbing. Fig. 10 shows the surfaces of three LAS-SiC composite samples, one in the as-ground condition (320 grit diamond), one after a ceraming treatment to a maximum 900° C temperature, and one after a 1050° C heat-treatment. After the 900° C, 2 h heat-treatment it appears a very thin glassy film covers the surface and makes the surface features appear rather diffuse. This glassy film may be a result of oxidation of the SiC fibres on the surface or may be residual glass exuded from the crystallized matrix. X-ray analysis indicates no difference between the surface of this sample and its interior, both showing only the  $\beta$ -quartz solid solution phase.

The surface of the sample heat-treated to 1050° C for 2 h in air is covered with a rather thick (20  $\mu$ m) glaze that, on cooling, appears to

have partially crystallized, as can be seen in Fig. 10. X-ray analysis of the sample surface indicates that, in addition to the  $\beta$ -quartz solid solution phase, there exists a substantial amount of  $\beta$ -spodumene-silica solid solution  $[(\text{Li}_2\text{O}, \text{MgO}) \cdot \text{Al}_2\text{O}_3 \cdot n\text{SiO}_2 (n > 3.5)]$ , or Keatite S.S. as it is sometimes called.

In addition to the surface formation, LAS-SiC samples air aged over 950° C also exhibit porosity formation within the matrix accompanied by a slight drop in bend strength. Fig. 11 shows this porosity formation for a sample aged for 100 h at 1000° C. This sample exhibited a loss in r.t. bend strength of ~ 20% as well. It appears that a rather low melting constituent of the LAS matrix is exuding from the interior to the surface of the composite, leaving behind porosity formation.

TABLE III Properties of 50 vol% SiC fibre reinforced LAS composites

Property	0°	0°/90°
Density (g cm <sup>-3</sup> )	2.5	2.5
Flexural strength (MPa)		
r.t.	600	380
800° C	800	410
1000° C	850	480
Fracture toughness - $K_{IC}$ (MN m <sup>-3/2</sup> )		
r.t.	17	10
1000° C	25	12
Thermal expansion (10 <sup>-6</sup> °C <sup>-1</sup> )	2.2	1.6 (90°)
Thermal conductivity (cal sec <sup>-1</sup> cm <sup>-1</sup> °C <sup>-1</sup> ) (W m <sup>-1</sup> K <sup>-1</sup> )	3.5 × 10 <sup>-3</sup> 1.465	3.5 × 10 <sup>-3</sup> 1.465

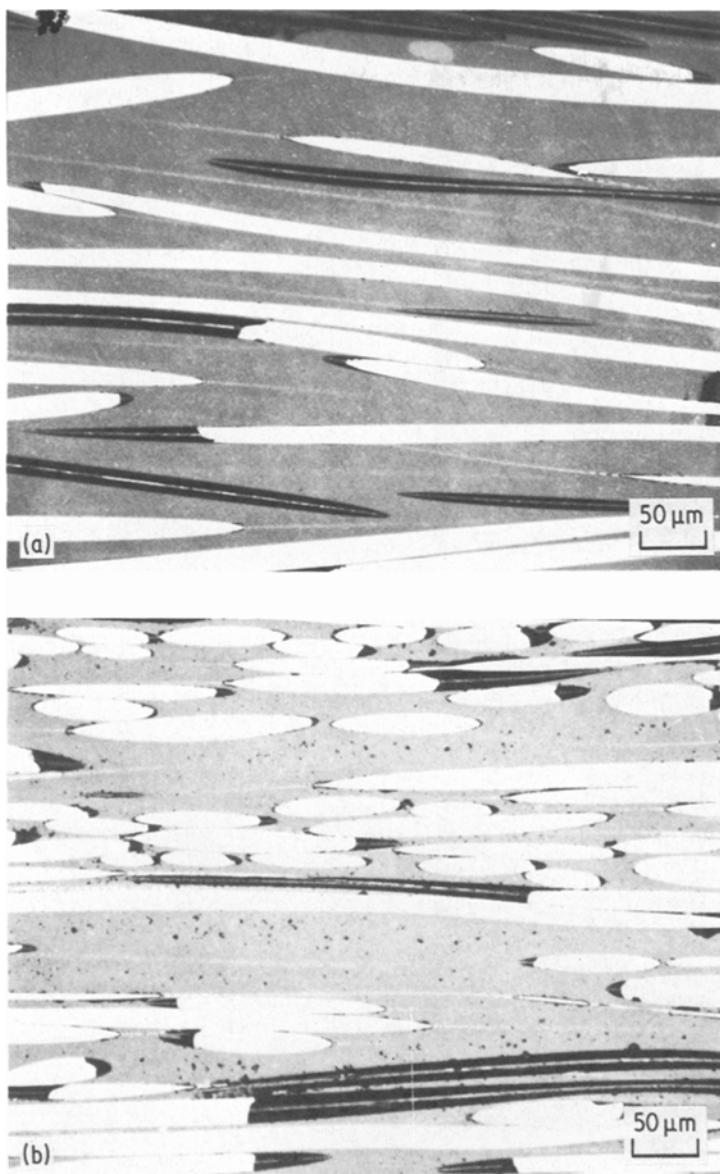


Figure 11 Longitudinal cross-sections of LAS-SiC composites (a) as-pressed and (b) after ageing in air for 100 h at 1000° C.

Since this phenomenon does not occur with monolithic Corning 9608 LAS, it must be caused as a result of the processing of the LAS into composite form.

A further phenomenon noticed when LAS-SiC samples are heat-treated in air above  $\sim 1000^{\circ}\text{C}$ , is the formation of a few rather large ( $30\ \mu\text{m}$ ) holes in the surface glaze, accompanied in some cases by bubble formation over the holes while the sample is at temperature. Fig. 12a shows the appearance of these holes on the surface of a sample heated to  $1050^{\circ}\text{C}$  for 2 h in air, while Fig. 12b shows the interior underneath one of these holes after  $\approx 100\ \mu\text{m}$  of the surface had been

ground off. From Fig. 12b, it appears that in a few areas near the surface within the LAS-SiC composite there is a reaction between the SiC fibres and the LAS matrix that produces a gaseous phase plus a low melting glassy phase that is partially blown out of the composite interior by the escaping gas.

The nature of the reaction responsible for this phenomenon has not been established. Since this gross matrix-fibre reaction appears to occur only in oxidizing environments, and not when the samples are heated in either Ar or vacuum, it may be related to the oxidation of the SiC fibres producing either volatile SiO and/or CO gas. Why this

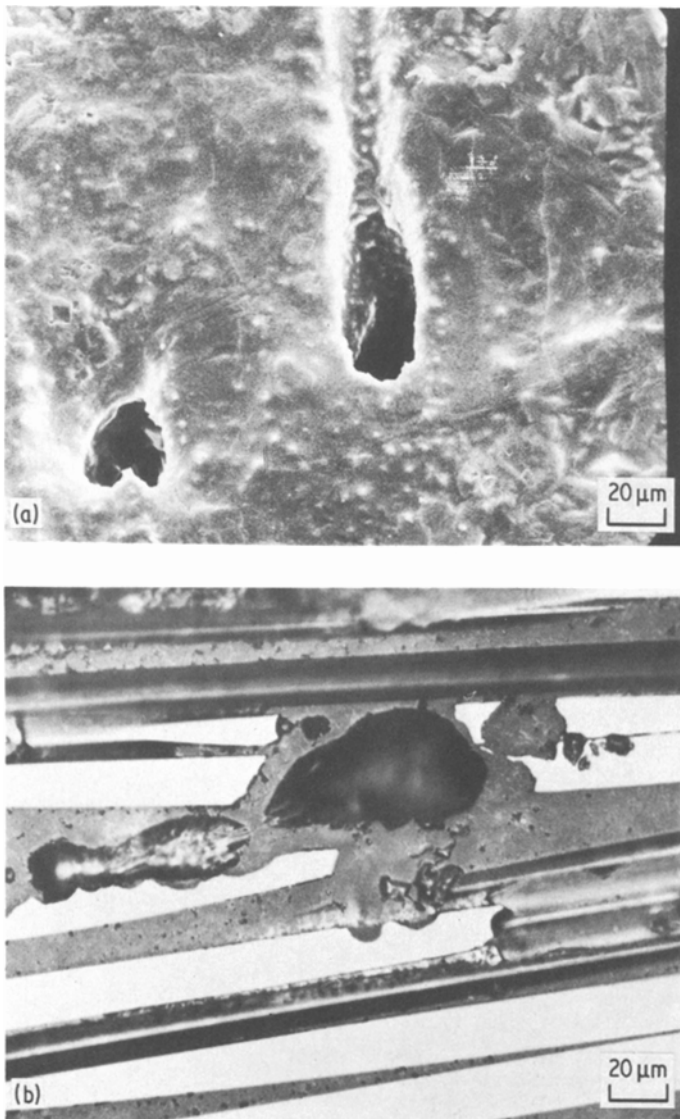


*Figure 12* LAS-SiC composite after 1050° C, 2 h, air-treatment showing (a) sample surface and (b) sample interior.

reaction appears to occur only at discrete areas on the sample and not over its entire surface is not known. The area of LAS-SiC composite oxidation is undergoing further study.

## 6. Conclusions

From the results of this investigation of the SiC fibre reinforced lithium aluminosilicate (LAS) glass-ceramic matrix composite system, it was demonstrated that LAS-SiC glass-ceramic composites can be fabricated that exhibit high strength and excellent toughness properties from r.t. to over 1000° C. In addition, these composite materials exhibit low density, low thermal expansion, and relatively low thermal conductivity. These properties are summarized in Table III. It was also found

that the LAS-SiC composite system exhibits good elevated temperature creep properties in bending to over 1000° C.

While further work in this system is necessary to resolve the questions concerning the high temperature oxidation behaviour, the extremely attractive strength, density, and, in particular, fracture toughness properties of the LAS-SiC fibre composite system make it ideally suited for potential application as a lightweight high temperature structural material.

## Acknowledgement

This work was supported by the Office of Naval Research under Contract number N00014-78-C-0503.

## References

1. K. M. PREWO and J. F. BACON, Proceedings of the Second International Conference on Composite Materials, Toronto, Canada, April 1978 (AIME, New York, 1978) p. 64.
2. K. M. PREWO, J. F. BACON and D. L. DICUS, *SAMPE Q.* (1979) 42.
3. K. M. PREWO, in "Proceedings of The Conference on Advanced Composites-Special Topics" (Technology Conferences, El Segundo, CA., 1979).
4. J. F. BACON and K. M. PREWO, Proceedings of the Second International Conference on Composite Materials, Toronto, Canada (AIME, New York, 1978) p. 753.
5. K. M. PREWO and J. J. BRENNAN, *J. Mater. Sci.* **15** (1980) 463.
6. *Idem*, *J. Mater. Sci.* **17** (1982) 1201.
7. W. F. BROWN, Jr. and J. E. SRAWLEY, "Plane Strain Crack Toughness Testing of High-Strength Metallic Materials", *Am. Soc. Test. Mat., S. T. P.* 410 (ASTM, Philadelphia, 1966) pp. 13-15.
8. H. KONISHI and T. CRUSE, *J. Comp. Mater.* **6** (1972) 114.
9. D. C. LARSON and J. W. ADAMS, "Property Screening and Evaluation of Ceramic Turbine Materials", Semiannual Interim Technical Report No. 8, Contract F33615-79-C-5100, June 1980.
10. R. A. SHAPERY, *J. Comp. Mater.* **2** (1968) 380.
11. P. W. McMILLAN, "Glass-Ceramics", Second Edition (Academic Press, London, England, 1979) p. 238.

*Received 1 December 1981  
and accepted 18 January 1982*